Bio-Design and Manufacturing (2022) 5:201–209
https://doi.org/10.1007/s42242-021-00156-1

RESEARCH ARTICLE

Epidermal self-powered sweat sensors for glucose and lactate monitoring

Xingcan Huang[1] · Jiyu Li[1] · Yiming Liu[1] · Tszhung Wong[1] · Jingyou Su[1] · Kuanming Yao[1] · Jingkun Zhou[1] · Ya Huang[1] · Hu Li[1] · Dengfeng Li[1] · Mengge Wu[1] · Enming Song[1] · Shijiao Han[2] · Xinge Yu[1]

Received: 19 April 2021 / Accepted: 23 June 2021 / Published online: 19 July 2021

Abstract

Sweat could be a carrier of informative biomarkers for health status identification; therefore, wearable sweat sensors have attracted significant attention for research. An external power source is an important component of wearable sensors, however, the current power supplies, i.e., batteries, limit further shrinking down the size of these devices and thus limit their application areas and scenarios. Herein, we report a stretchable self-powered biosensor with epidermal electronic format that enables the in situ detection of lactate and glucose concentration in sweat. Enzymatic biofuel cells serve as self-powered sensing modules allowing the sweat sensor to exhibit a determination coefficient (R^2) of 0.98 with a sensitivity of 2.48 mV/mM for lactate detection, and R^2 of 0.96 with a sensitivity of 0.11 mV/μM for glucose detection. The microfluidic channels developed in an ultra-thin soft flexible polydimethylsiloxane layer not only enable the effective collection of sweat, but also provide excellent mechanical properties with stable performance output even under 30% stretching. The presented soft sweat sensors can be integrated at nearly any location of the body for the continuous monitoring of lactate and glucose changes during normal daily activities such as exercise. Our results provide a promising approach to develop next-generation sweat sensors for real-time and in situ sweat analysis.

Graphic abstract

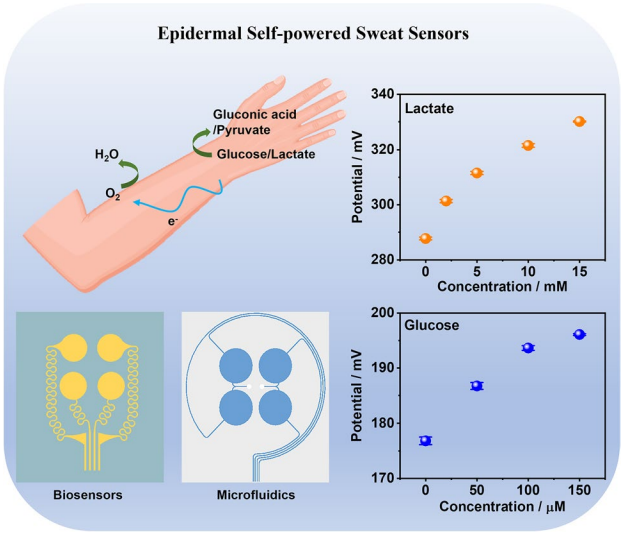

Keywords Sweat sensor · Self-powered · Epidermal electronics · Enzymatic biofuel cells · Microfluidics

Xingcan Huang, Jiyu Li, and Yiming Liu have contributed equally to this work.

✉ Xinge Yu
xingeyu@cityu.edu.hk

[1] Department of Biomedical Engineering, City University of Hong Kong, Hong Kong 999077, China

[2] School of Computer Science and Engineering, University of Electronic Science and Technology of China, Chengdu 610054, China

Introduction

The development of wearable electronics, especially thin and stretchable devices, is increasingly attractive due to their promising applications in health monitoring and early disease diagnostics. Recent advances of skin-integrated electronics in biophysical signal measurements of temperature [1], pulse waves [2], and electrocardiographs (ECG) [3, 4] have highlighted the importance of device geometries and mechanics. Regarding the measurements of biochemical signals, parameters of human sweat, including glucose, lactate, pH, and inorganic ion levels have shown great relevance to physiological information and therefore have attracted great attention for research [5–8]. Sweat sensing is a non-invasive approach of body fluid analysis that can monitor the chemical signals of the body and thus reveal the health status [5, 9]. Traditional sweat analysis methods mainly rely on collecting sweat by gauze pads taped to skin and screening biomarkers by benchtop instruments, however, these are complex and time consuming. There is a lack of miniaturized portable instruments for direct sweat collection and in situ analysis of multiple biomarkers in sweat, which limits the practical development of sweat analysis in the area of health monitoring [5, 7]. Hence, innovation in wearable devices for in situ sweat collection and analysis has been urgent. Furthermore, irrespective of application, the lack of suitable power sources is a significant obstacle for wearable electronics, as the weight and volume of batteries would largely influence their miniaturization, flexibility, and biocompatibility [10–13]. To date, great efforts have been directed toward wearable self-powered sensors, such as flexible triboelectric nanogenerators [14–16] and piezoelectric nanogenerators [17–19]. These self-powered technologies enable the conversion of mechanical energy from body motions to sensing signal outputs, thus providing an alternative pathway for wearable power management. For self-powered biosensors aimed at sweat monitoring, enzymatic biofuel cells (EBFCs) could be an ideal candidate by catalyzing the redox reaction of biofuels to generate electricity [5, 10, 20–22]. In such system, the oxidation of biofuels would occur on the bioanodes and electrons would be released. Meanwhile, oxygen would be reduced to water on the cathode. As enzymes have specific catalytic ability for targets, the catalyst reaction would not be disturbed by other interferences and their catalytic activity would be retained for several weeks at room temperature with good reusability [5, 6, 9, 23, 24]. The electrical outputs generated by EBFCs are proportional to the ingredient concentration and therefore allow them to serve as biosensors [5, 25–28]. Consequently, the question arises as to whether we can integrate EBFCs with microfluidic channels into a thin and soft format for a self-powered wearable sweat sensing device.

In the present work, we report a class of materials, mechanics, and microfluidic designs in skin-integrated electronics for self-powered, real-time sweat sensing technology. The self-powering sensors associate with lactate and glucose EBFCs that are constructed on a stretchable circuit support by a thin soft polydimethylsiloxane (PDMS)-based microfluidic system for monitoring lactate and glucose concentration in sweat. PDMS is a commonly used substrate material for skin-integrated electronics due to its excellent mechanical properties, stable chemical/physical nature, and safety to skin [5, 9, 29]. The real-time detection of changes in lactate concentration, which could indicate physical stress, may help to identify transitions from aerobic to anaerobic states [23, 30], while measuring the variation of glucose level in sweat may consist the means of tracking blood glucose levels [31, 32]. In this work, graphene spray-coated on gold is proposed for better stretchability and a more homogeneous distribution than the application of a drop casting method. Compared with other self-powered biosensors, especially for sensors based on biofuel cells, an integrated device with microfluidics technology could collect sweat in situ and gather the concentration data of lactate and glucose with excellent stretchability and flexibility [33–36] and would in turn have wide application prospects in the real-time monitoring of health status during daily life activities.

Materials and methods

Fabrication of stretchable self-powered lactate and glucose sensors

The fabrication process of the stretchable self-powered biosensor was started on quartz glass, which was firstly cleaned by acetone, ethanol, and deionized water (DI water, > 18 MΩ cm) sequentially. Next, poly(methylmethacrylate) (PMMA) solution (20 mg/mL, chlorobenzene solvent) was spun-coated on the glass and baked at 200 °C for 20 min to form a sacrificial layer for the transfer printing process. Subsequently, poly(pyromellitic dianhydride-co-4,4′-oxydianiline), amic acid solution (Sigma-Aldrich) was spin-coated on the PMMA film and baked at 250 °C for 30 min to form a thin polyimide (PI, 2 μm) layer. A thickness of 30 nm Cr and 180 nm Au were sequentially deposited on the PI film via electron-beam evaporation. Next, the flexible circuits were defined by photolithography as follows: first, photoresist coating (PR, AZ 5214, AZ Electronic Materials, USA) was applied at 3000 r/min for 30 s followed by soft bake at 110 °C for 5 min; then, the PR pattern was defined by ultraviolet light exposure for 5 s and rinsing in the developer solution (AZ 300MIF) for 60 s defined the PR pattern; subsequently, wet etching by

gold etchant (iodine (I_2)/potassium iodide (KI) solution) for 90 s and rinsing by acetone and DI water to remove the residual PR [37]. The stretchable serpentine interconnects were defined by the dry etching of PI by reactive ion etching (RIE, Oxford Plasma-Therm 790 RIE system) with oxygen gas under 200 W RF power for 8 min. Following immersion in acetone for 12 h to remove the sacrificial layer, the pattern was picked up by poly(vinyl alcohol) (PVA) tapes for transfer printing. A thin stretchable PDMS layer (170 μm, 30:1, Sylgard 184, Dow Corning Corporation, USA) served as the receiving substrate, which was fabricated by spin-coating at 600 r/min for 30 s and baking at 110 °C for 5 min. Prior to the transfer printing process, the PVA tape and PDMS substrate were exposed to UV-ozone (UVO) for 5 min to create chemical groups enhancing the bonding strength. Then, the PVA tape was attached on the PDMS substrate and the sample was immersed in water to remove PVA and form the stretchable electrodes and interconnects.

For the biofuel cell-based biosensors part, 50 μL graphene suspension (5 mg/mL, ethanol solvent) was spray-coated on the prepared four Au electrodes on a 100 °C hot plate for accelerating the volatilization of ethanol and the immobilization of graphene. Here, the graphene layer served as a host for enzymes and the electron transfer channel from enzymes to electrode. The graphene-coated electrodes were then treated with UVO for 5 min to improve their hydrophilicity. The catalytic inks of bioanodes were prepared by sequentially mixing 2 μL lactate oxidase (LO*x*, 1 U/μL) or glucose oxidase (GO*x*, 2.5 U/μL), 1 μL bovine serum albumin (BSA, 10 mg/mL) and 2 μL glutaraldehyde (2% w/v). The catalytic ink of biocathodes was prepared by a similar procedure, but replacing oxidases with laccase (Lac). After dropping catalytic inks on the graphene layer and drying in a refrigerator at 4 °C, 2 μL chitosan (1% w/v) was dropped onto the enzyme-coated electrode for encapsulation. Finally, the obtained biosensors were stored in the refrigerator overnight.

Fabrication of flexible microfluidic device

The fabrication of microfluidic system was based on photolithography and replica molding of PDMS. Firstly, the mold was developed by patterning SU-8 photoresist (SU-8 2015, Microchem) with a thickness of 30 μm on a 4″ silicon wafer, which was sequentially cleaned by isopropyl alcohol, acetone, DI water and a final rinse with isopropyl alcohol. After baking at 95 °C for 5 min on a hot plate, the baked SU-8 photoresist with silicone wafer was exposed to UV light through mounting to a photomask, followed by post baking at 95 °C for 3 min. The exposed substrate was immersed in the developer solution (SU-8 developer, Microchem) for 5 min to remove any unexposed photoresist. The mold was salinized by depositing a molecular layer of Trichloro (1*H*,1*H*,2*H*,2*H*-perfluorooctyl) silane (Sigma-Aldrich, St. Louis, MO, USA) to facilitate the release of PDMS from the mold master in the later steps. After the mold fabrication, the PDMS monomer was mixed with the curing agent in a weight ratio of 20:1; and the mixture was degassed in a vacuum environment for 3–5 min. The degassed PDMS mixture was poured onto the control layer mold with a thickness of 150 μm. After baking in an oven at 80 °C for 20 min, the PDMS substrate was chopped and peeled off its mold. The inlet was obtained by punching holes of 0.5 mm diameter, and the outlet was fabricated by cutting the extra PDMS at the end of the microchannels. The PDMS substrate was finally bonded onto the self-powered sensor module layer using oxygen plasma treatment (energy: 5 kJ; Harrick plasma cleaner PDC002) for further sweat collection and analysis.

Characterization

The material and electrode surface characterization tasks were performed by scanning electron microscopy (SEM, FEI Quanta 250). The open-circuit potential (OCP) was measured by the data acquisition (DAQ)/multimeter system (PowerLab 16/35, AD Instruments) with a constant sampling frequency of 100 Hz. The polarization curve of biofuel cells was evaluated by the I/V measurement from OCP to zero by a Keysight B1500A semiconductor analyzer. The current density was calculated through the electrode area (0.07065 cm^2), and the power density was obtained by multiplying current density by potential. The device testing procedure on volunteers was conducted with their full informed consent.

Results and discussion

Epidermal stretchable self-powered biosensor for sweat monitoring

The schematic diagram of a stretchable epidermal self-powered sweat sensor is illustrated in Fig. 1a, which consists of four self-power biosensors and a microfluidics system. As shown in Figs. 1a and 1b, the construction of biosensors adopts a multilayer stacking layout. A thin soft PDMS layer (170 μm) serves as the substrate, and Au electrodes with serpentine traces (180 nm) supported by a 2 μm thick PI define the stretchable electrodes and connection cables. In the biosensors, the catalyst layer includes enzymes and sprayed graphene, which is responsible for catalyzing the reactions of lactate, glucose, and oxygen, and thus generating electricity. Another layer of PI (2 μm thick) on top of the Au circuits serves as encapsulation for short circuit prevention. The pads in the biosensor's response for the catalyst are

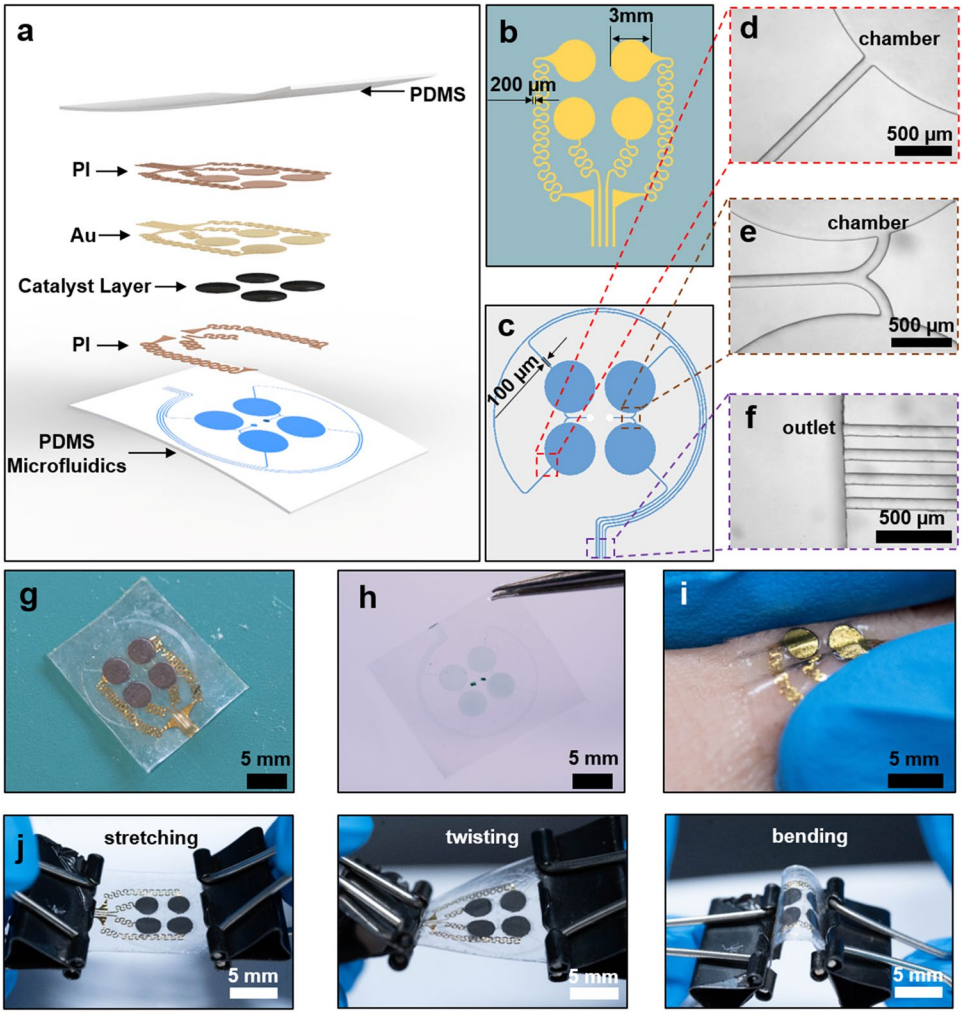

Fig. 1 Overview of the epidermal and stretchable self-powered sweat sensor. **a** Schematic illustration of a self-powered sweat sensor for lactate and glucose analysis. **b**, **c** Design sketches of the sweat sensor and the microfluidic system. **d**–**f** Micrographs of the chamber outlet, chamber inlet and the overall outlet of the microfluidic system. **g**, **h** Optical images of the self-powered sensor and the microfluidic system. **i** Optical image of the device attached to the back of hands. **j** Optical images of the biosensor under stretching, twisting, and bending

designed with a diameter of 3 mm, while the interconnecting filamentary serpentine has a line width of 200 μm. The serpentine interconnection and island-bridge design utilize the mechanical guidelines in stretchable electronics and therefore greatly enhance the stretchability of the sweat sensors. Figures 1a and 1c show the design of the microfluidic system, where the microchannels are developed on a PDMS thin layer with a channel width of 100 μm that can collect sweat directly from the skin. Two separate inlets of the microfluidic system allow sweat to accumulate and flow to the corresponding bioanodes and biocathode in different chambers for lactate and glucose sensing (Fig. 1e). Subsequently, sweat flows out of the chambers via the microchannels and gathers to the outlet (Figs. 1d and 1f). The overall dimension of the integrated device is 15 mm × 10 mm × 0.34 mm (length × width × thickness) and its weight is only 90 mg, showing the ultra-thin and light-weighted features, which enable conformal and tight attachment to the human skin (Figs. 1g–1i and S1) [38]. Furthermore, as the biosensor and microfluidic system are both constructed on the soft and ultra-thin PDMS substrate, the integrated device can be stretched, twisted (over 45°), and bent (over 15°) to accommodate realistic body motions (Fig. 1j).

Self-powered biosensor characterization

The enzymatic biofuel cell design plays an essential role in achieving self-powering behaviors. The principles and schematic illustrations of the biofuel cell-based biosensors are shown in Fig. 2a. In the bioanode, lactate in sweat is oxidized by LO*x* into pyruvate, while GO*x* oxidizes glucose into gluconic acid. At the same time, electrons are released in the oxidation reaction. In the biocathode, oxygen is reduced into water (H_2O) by Lac and electrons are obtained. As a result, the OCP values of EBFCs exhibit strong correlation with the lactate or glucose concentration in sweat. As shown in Figs. 2b and S2a, the distribution of spray-coated graphene on the metallic electrodes is highly uniform and thus guarantees the great sensing uniformity. Here, distributed graphene facilitates the electron transfer between the active center of enzymes and metallic electrode surfaces. After UVO treatment, catalytic ink becomes well-dispersed

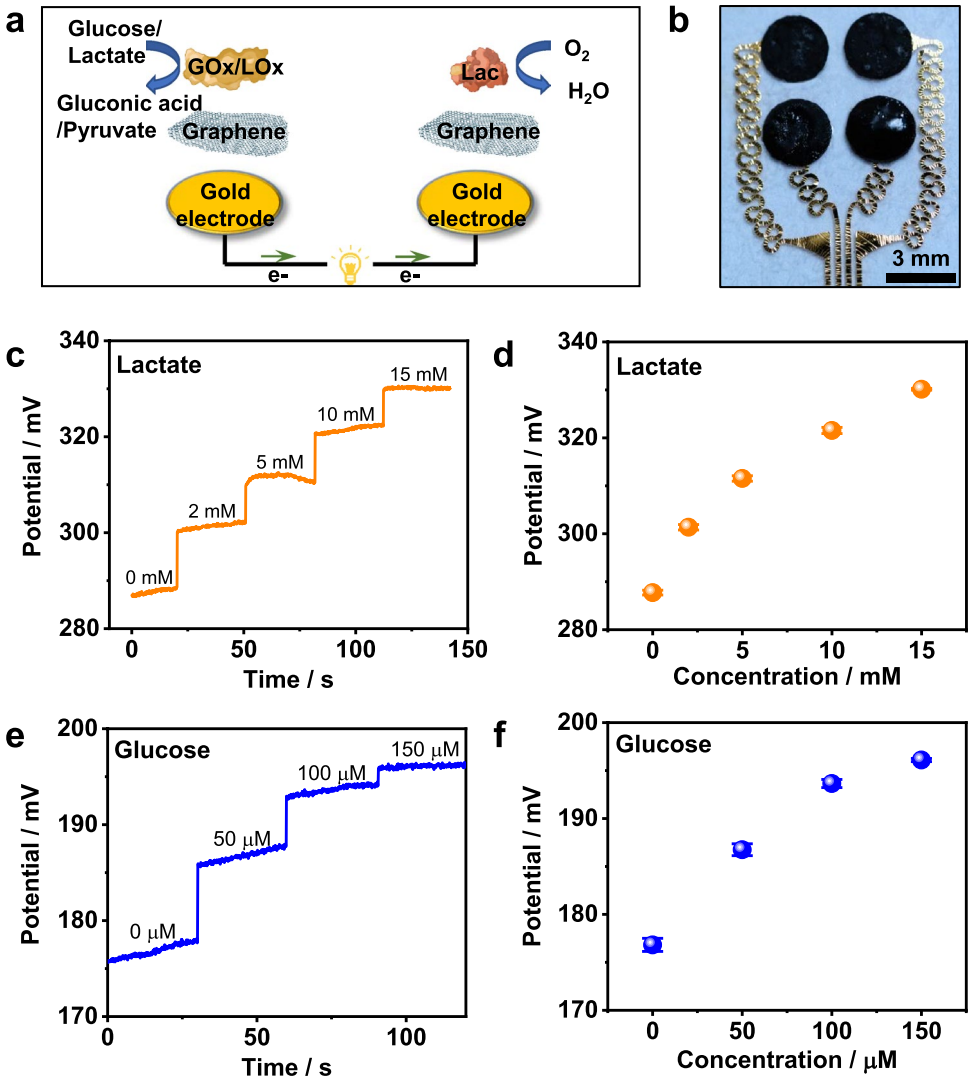

Fig. 2 Electrical characterizations of the self-powered sensors. **a** Schematic illustration of the biofuel cell-based biosensor. **b** Enlarged optical image of the biosensor device. **c** Real-time electrical response of the sensor to various lactate concentrations and **d** the corresponding calibration curve. **e** Real-time electrical response of the sensor to various glucose concentrations in phosphate buffer and **f** the corresponding calibration curve

and enzymes can be tightly immobilized on the graphene layer (Figs. 2b and S2b–S2d). Figures 2c–2f show the performance of the self-powered sensors in lactate and glucose sensing. As illustrated in Fig. 2c, the OCP of the lactate EBFCs increases with the rise of lactate concentration in the electrolyte (0.01 M phosphate buffered saline (PBS) buffer), indicating that the biosensor has good response to lactate concentrations ranging from 0 to 15 mM. Figure 2d presents the OCP of the sensor as a function of various concentrations of lactate, revealing an apparent linear relationship between the OCP of lactate concentration. The sensitivity of 2.48 mV/mM and the determination coefficient (R^2) of 0.98 in the lactate EBFCs show the excellent performance of the lactate sensor. Figure 2e depicts the representative OCP responses of glucose EBFCs for glucose in the PBS buffer for 0–150 μM glucose concentrations in the solution. Similarly to the lactate sensors, a linear relationship between the OCP and glucose concentration with a sensitivity of 0.11 mV/μM and an R^2 of 0.96 can be obtained, indicating the great performance of the glucose sensors.

Characterization of mechanical properties

In order to investigate the mechanical properties of the self-powered biosensors, a comprehensive characterization of the device is conducted herein, involving the study of OCP, current density and power density versus various stretching strains (from 0 to 30%). Since 30% is the typical maximum strain level for the human skin, we only study the performance differences of the sensors under 30% stretching [15, 39]. Figure 3a shows the optical images of the device under 0%, 10%, 20%, and 30% stretching, which indicate that no fractures and breaks occur to the interconnects due to the advanced serpentine design. Figures 3b–3e depict the electrical outputs of lactate and glucose sensing in the device under different stretching levels. The concentration of lactate and glucose are fixed at 15 mM and 150 μM, respectively.

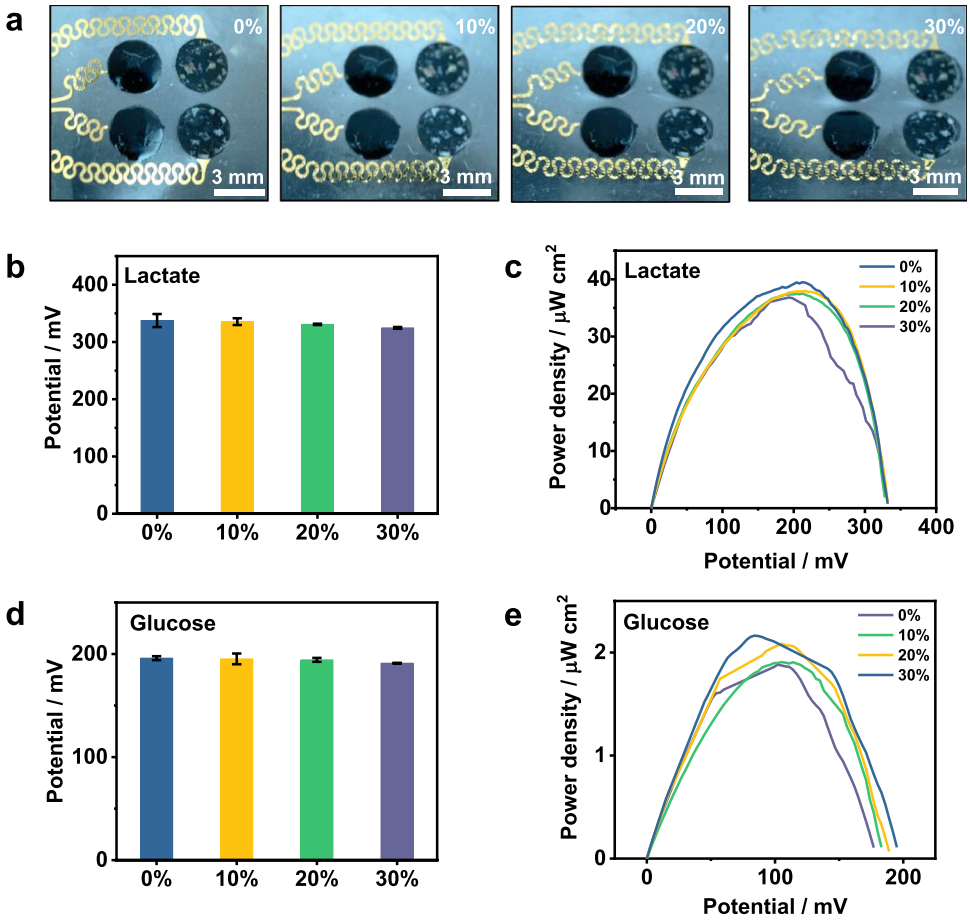

Fig. 3 Mechanical characterizations of the self-powered sensors. **a** Optical images of the self-powered biosensor under 0%, 10%, 20%, and 30% stretching. **b**, **c** Open-circuit potential and power density of the lactate biofuel cell under 0%, 10%, 20%, and 30% stretching in 15 mM lactate electrolyte. **d**, **e** Open-circuit potential and maximum power density of the glucose biofuel cell under 0%, 10%, 20%, and 30% stretching in 150 μM glucose electrolyte

The corresponding OCP of the devices without any stretching is 337.4 mV for lactate sensors and 195.8 mV for glucose sensors, with a maximum current density (MCD) and power density (MPD) of 644.7 μA/cm^2 and 39.5 μW/cm^2 for lactate sensors and 41.5 μA/cm^2 and 2.16 μW/cm^2 for glucose sensors, respectively (Figs. S3 and 3). Hardly any change of OCP can be found in these sensors when the stretching level is less than 20%, while 30% stretching only causes negligible OCP reduction. As a result, the OCP and MPD of the devices exhibit highly stable behaviors even under stretching states, specifically, values of 324.68 mV, 36.8 μW/cm^2 and 191.08 mV, 1.9 μW/cm^2 respectively for lactate and glucose sensors under 30% stretching. Both OCP and MPD for lactate and glucose sensors can maintain over 88% of their performance under 30% stretching as compared to the initial values without stretching.

Microfluidic device design and characterization

In the proposed design, a microfluidic system serves as the on-skin sweat collection platform that contains two regions with two chambers (3 mm in diameter) for lactate and glucose sensing each and a microchannel of 100 μm width for sweat flowing (Fig. S4a). The inlet channel with a diameter of 0.5 mm connects the microchambers to allow sweat flowing in (Fig. S4b). Generally, this hole diameter can cover 2–3 sweat glands on the palm based on estimation [40]. Therefore, sweat could be drawn into the microchannel by hydraulic pressure from osmolality differences between sweat and plasma created by glands [41], and the collected sweat fluid guided through a bifurcation nozzle could in turn flow to each chamber. The rate of sweat fluid flow through each chamber is the same due to the symmetrical design, thus enabling the analysis of lactate and glucose with high time consistency [5, 29]. The computational analysis (COMSOL Multiphysics, COMSOL, Burlington, MA) of the velocity profiling of the sweat fluid going through bifurcation shows a homogeneous distribution, allowing for a similar rate of sweat fluid flow from the skin into the microchambers (Fig. S4c). The circle shape design of the microchamber can avoid the formation of 'dead space' during air degassing, leading to more accurate analysis. As shown in Fig. S4d, the result of simulated 3D velocity of the sweat fluid going through the microchannel indicates that the sweat fluid always flows along the center of the microchannel without any shifting

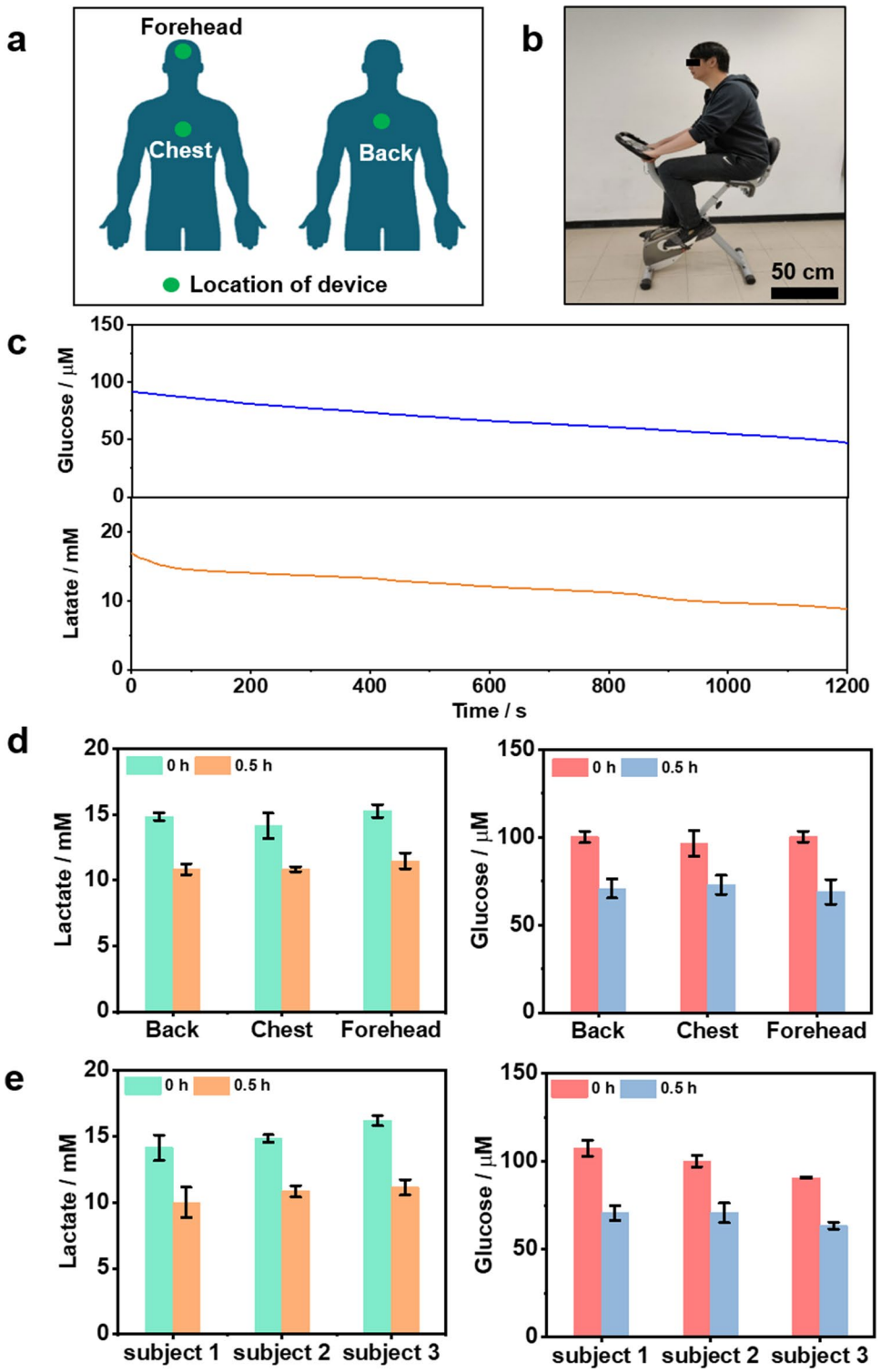

Fig. 4 On-body real-time perspiration analysis. **a** Schematic Illustration of the sensors mounted on various locations of a test subject. **b** Optical image of the test subject on a stationary cycling. **c** Continuous monitoring of lactate and glucose concentration in perspiration during exercise. **d** Comparison of lactate and glucose concentration in perspiration applied to different body location during exercise. **e** Comparison of lactate and glucose concentration in perspiration attached on the back of different subjects during exercise

movement. As illustrated in Fig. S5, we also recorded the air degassing procedure; nearly 99% of the area could be filled by sweat fluid within 1 min and air could be removed entirely at 33 min. Therefore, this microfluidic system allows the efficient collection of sweat.

In situ and real-time sweat analysis

The epidermal self-powered sweat sensors were tested on the human body for in situ and real-time sweat analysis. As shown in Fig. 4a, the soft sweat sensors can be attached in various body locations, including the forehead, chest, and

back. Real-time lactate and glucose concentration monitoring could be performed on a subject during constant-load exercise on a cycle ergometer, as shown in Fig. 4b. Figure 4c presents the glucose and lactate concentration data in real-time for the testing subject during exercise for 1200 s, where the sweat sensors are attached to the back of the subject. During the exercise, with continued perspiration, the glucose and lactate concentration both gradually decreased, which is due to the dilution effect of the increase of sweat rate [6, 41]. In addition, the lactate and glucose concentrations were measured in three different body locations (Fig. 4a) after 0.5 h of continuous exercise, with the results summarized in Fig. 4d. The figure compares these levels with their initial levels before exercise. The concentrations of lactate and glucose at different body areas were almost the same on different test locations, and obvious decrease could be found after 0.5 h of perspiration. Next, the change of lactate and glucose levels in the sweat were tested on three subjects during exercise by attaching the sensor to the back of volunteers to identify its universality (Fig. 4e). Obviously, the change trends of lactate and glucose levels were similar for different subjects. These results indicate that the soft self-powered biosensor exhibits great effectiveness and application potential for in situ and real-time sweat analysis.

Conclusions

In this paper, we have presented a newly developed epidermal, stretchable self-powered biosensor to achieve the in situ detection of lactate and glucose concentrations in human sweat. A careful selection of materials and device structures enables biofuel cells serving as accurate sensing components to avoid using additional power supplies. The combination of an advanced mechanical design consisting of stretchable electronics, a microfluidic system, and biosensors allows the self-powered sweat sensing device to exhibit excellent sweat collection capability and sensing accuracy even under great levels of stretching. Measurements by the sensors on volunteers show the real-time response to lactate and glucose level changes, indicating the application potential of the proposed biosensor in wearable sweat sensing and healthcare monitoring scenarios.

Supplementary Information The online version contains supplementary material available at https://doi.org/10.1007/s42242-021-00156-1.

Acknowledgements This work was supported by the City University of Hong Kong, China (Nos. 9610423, 9667199, and 9667221), Research Grants Council of the Hong Kong Special Administrative Region, China (No. 21210820), Shenzhen Science and Technology Innovation Commission, China (No. JCYJ20200109110201713), Science and Technology of Sichuan Province, China (No. 2020YFH0181), and China Postdoctoral Science Foundation (No. 2019TQ0051).

Author contributions XCH was involved in data curation, formal analysis, investigation, methodology, writing—original draft; JYL and YML was involved in conceptualization; THW and JYS contributed to methodology; KMY contributed to visualization; JKZ, YH, HL, DFL, and MGW were involved in software and data analysis; EMS was involved in data curation, formal analysis and supervision; SJH contributed to funding acquisition and project administration; XGY contributed to conceptualization, funding acquisition, project administration, resources, supervision and writing—review and editing.

Declarations

Conflict of interest The authors declare that there is no conflict of interest.

Ethical approval All procedures were followed in accordance with the ethical standards of the responsible committee on human experimentation (institutional and national) and with the Helsinki Declaration of 1795, as revised in 2008 (5). The informed consent of all patients was obtained prior inclusion in the study.

References

1. Crawford KE, Ma YJ, krishnan S, et al (2018) Advanced approaches for quantitative characterization of thermal transport properties in soft materials using thin, conformable resistive sensors. Extreme Mech Lett 22:27–35. https://doi.org/10.1016/j.eml.2018.04.002
2. Schwartz G, Tee CKB, Mei J et al (2013) Flexible polymer transistors with high pressure sensitivity for application in electronic skin and health monitoring. Nat Commun 4:1859
3. Chung HU, Bong HK, Jong YL et al (2019) Binodal, wireless epidermal electronic systems with in-sensor analytics for neonatal intensive care. Science 363:6430. https://doi.org/10.1126/science.aau0780
4. Li D, Yao K, Gao Z et al (2021) Recent progress of skin-integrated electronics for intelligent sensing. Light Adv Manuf 2:1–20
5. Bandodkar AJ, Gutruf P, Choi J et al (2019) Battery-free, skin-interfaced microfluidic/electronic systems for simultaneous electrochemical, colorimetric, and volumetric analysis of sweat. Sci Adv. https://doi.org/10.1126/sciadv.aav3294
6. Gao W, Emaminejad S, Nyein HYY et al (2016) Fully integrated wearable sensor arrays for multiplexed in situ perspiration analysis. Nature 529:509–514. https://doi.org/10.1038/nature16521
7. Koh A, Kang D, Xue Y et al (2016) A soft, wearable microfluidic device for the capture, storage, and colorimetric sensing of sweat. Sci Transl Med. https://doi.org/10.1126/scitranslmed.aaf2593
8. He W, Wang C, Wang H et al (2019) Integrated textile sensor patch for real-time and multiplex sweat analysis. Sci Adv. https://doi.org/10.1126/sciadv.aax0649
9. Yu Y, Nassar J, Xu C et al (2020) Biofuel-powered soft electronic skin with multiplexed and wireless sensing for human–machine interfaces. Sci Robot 5:41. https://doi.org/10.1126/scirobotics.aaz7946
10. Huang X, Zhang L, Zhang Z et al (2019) Wearable biofuel cells based on the classification of enzyme for high power outputs and lifetimes. Biosens Bioelectron 124–125:40–52. https://doi.org/10.1016/j.bios.2018.09.086

11. Yu X, Xie Z, Rogers JA et al (2019) Skin-integrated wireless haptic interfaces for virtual and augmented reality. Nature 575:473–479. https://doi.org/10.1038/s41586-019-1687-0
12. Liu Y, Zheng H, Zhao L et al (2020) Electronic skin from high-throughput fabrication of intrinsically stretchable lead zirconate titanate elastomer. Research. https://doi.org/10.34133/2020/1085417
13. Liu Y, Wang L, Zhao L et al (2020) Recent progress on flexible nanogenerators toward self-powered systems. Information 2:318–340. https://doi.org/10.1002/inf2.12079
14. Wu M, Gao Z, Hou S et al (2021) Thin, soft, skin-integrated foam-based triboelectric nanogenerators for tactile sensing and energy harvesting. Mater Today Energy 20:100657. https://doi.org/10.1016/j.mtener.2021.100657
15. Yao K, Liu Y, Li D et al (2020) Mechanics designs-performance relationships in epidermal triboelectric nanogenerators. Nano Energy 76:105017. https://doi.org/10.1016/j.nanoen.2020.105017
16. He J, Xie Z, Yao K et al (2021) Trampoline inspired stretchable triboelectric nanogenerators as tactile sensors for epidermal electronics. Nano Energy 81:105590. https://doi.org/10.1016/j.nanoen.2020.105590
17. Wang ZL, Song J (2006) Piezoelectric nanogenerators based on zinc oxide nanowire arrays. Science 312:242–246. https://doi.org/10.1126/science.1124005
18. Gao PX, Song JL, Wang ZL et al (2007) Nanowire piezoelectric nanogenerators on plastic substrates as flexible power sources for nanodevices. Adv Mater 19(1):67–72. https://doi.org/10.1002/adma.200601162
19. Yang L, Zhao Q, Chen K et al (2020) PVDF-based composition-gradient multilayered nanocomposites for flexible high-performance piezoelectric nanogenerators. ACS Appl Mater Interfaces 12(9):11045–11054. https://doi.org/10.1021/acsami.9b23480
20. Huang X, Zhang J, Su H et al (2021) Exploring the shape and distribution of electrodes in membraneless enzymatic biofuel cells for high power output. Int J Hydrogen Energy 46(33):17414–17420. https://doi.org/10.1016/j.ijhydene.2021.02.150
21. Zhang J, Huang X, Zhang L et al (2020) Layer-by-layer assembly for immobilizing enzymes in enzymatic biofuel cells. Sustain Energy Fuels 4:68–79. https://doi.org/10.1039/c9se00643e
22. Wu M, Yao K, Li D et al (2021) Self-powered skin electronics for energy harvesting and healthcare monitoring. Mater Today Energy. https://doi.org/10.1016/j.mtener.2021.100786
23. Jia W, Bandodkar JB, Valdés-Ramírez G et al (2013) Electrochemical tattoo biosensors for real-time noninvasive lactate monitoring in human perspiration. Anal Chem 85:6553–6560. https://doi.org/10.1021/ac401573r
24. Yang HW, Hua MY, Chen SL et al (2013) Reusable sensor based on high magnetization carboxyl-modified graphene oxide with intrinsic hydrogen peroxide catalytic activity for hydrogen peroxide and glucose detection. Biosens Bioelectron 41:172–179. https://doi.org/10.1016/j.bios.2012.08.008
25. Newman JD, Turner AP (2005) Home blood glucose biosensors: a commercial perspective. Biosens Bioelectron 20:2435–2453. https://doi.org/10.1016/j.bios.2004.11.012
26. Jeerapan I, Sempionatto JR, Wang J (2020) On-body bioelectronics: wearable biofuel cells for bioenergy harvesting and self-powered biosensing. Adv Func Mater 30:1906243. https://doi.org/10.1002/adfm.201906243
27. Ming Z, Wang J (2012) Biofuel cells for self-powered electrochemical biosensing and logic biosensing: a review. Electroanalysis 24:197–209. https://doi.org/10.1002/elan.201100631
28. Mercier P, Wang J (2020) Powered by sweat: throw out the batteries: biofuels will change the future of wearable devices. IEEE Spectr 57:28–33. https://doi.org/10.1109/MSPEC.2020.9126108
29. Ghaffari R, Choi J, Raj MS et al (2020) Soft wearable systems for colorimetric and electrochemical analysis of biofluids. Adv Funct Mater 30:37. https://doi.org/10.1002/adfm.201907269
30. Martin A, Kim J, Kurniawan JF et al (2017) Epidermal microfluidic electrochemical detection system: enhanced sweat sampling and metabolite detection. ACS Sens 2:1860–1868. https://doi.org/10.1021/acssensors.7b00729
31. Abellan-Llobregat A, Jeerapan I, Bandodkaret A et al (2017) A stretchable and screen-printed electrochemical sensor for glucose determination in human perspiration. Biosens Bioelectron 91:885–891. https://doi.org/10.1016/j.bios.2017.01.058
32. Kudo H, Sawada T, Kazawa E et al (2006) A flexible and wearable glucose sensor based on functional polymers with soft-MEMS techniques. Biosens Bioelectron 22:558–562. https://doi.org/10.1016/j.bios.2006.05.006
33. Gong S, Du S, Kong J et al (2020) Skin-like stretchable fuel cell based on gold-nanowire-impregnated porous polymer scaffolds. Small 16:e2003269. https://doi.org/10.1002/smll.202003269
34. Jia W, Valdés-Ramírez G, Bandodkar AJ et al (2013) Epidermal biofuel cells: energy harvesting from human perspiration. Angew Chem Int Ed Engl 52:7233–7236. https://doi.org/10.1002/anie.201302922
35. Yin S, Jin Z, Miyake T (2019) Wearable high-powered biofuel cells using enzyme/carbon nanotube composite fibers on textile cloth. Biosens Bioelectron 141:111471. https://doi.org/10.1016/j.bios.2019.111471
36. Zhang J, Liu J, Su H et al (2021) A wearable self-powered biosensor system integrated with diaper for detecting the urine glucose of diabetic patients. Sens Actu B Chem 341:130046. https://doi.org/10.1016/j.snb.2021.130046
37. Li D, Wang S, He J et al (2021) Bioinspired ultrathin piecewise controllable soft robots. Adv Mater Technol 6(5):2001095. https://doi.org/10.1002/admt.202001095
38. Liu Y, Wang L, Zhao L et al (2019) Thin, skin-integrated, stretchable triboelectric nanogenerators for tactile sensing. Adv Electron Mater 6:1901174. https://doi.org/10.1002/aelm.201901174
39. Arumugam V, Naresh MD, Sanjeevi R (1994) Effect of strain-rate on the fracture-behavior of skin. J Biosci 19:307–313. https://doi.org/10.1007/Bf02716820
40. Gray H, Goss C (1973) Anatomy of the human body, 29th American ed. Lea Febiger 42:488–499. https://doi.org/10.1136/pgmj.42.493.734-b
41. Sonner Z, Wilder E, Heikenfeld J et al (2015) The microfluidics of the eccrine sweat gland, including biomarker partitioning, transport, and biosensing implications. Biomicrofluidics 9:031301. https://doi.org/10.1063/1.4921039